Ion irradiation of inhomogeneous Schottky barriers on silicon carbide

F. Roccaforte,[a] S. Libertino, F. Giannazzo, C. Bongiorno, F. La Via, and V. Raineri
Consiglio Nazionale delle Ricerche - Istituto per la Microelettronica e Microsistemi (CNR-IMM), Sezione di Catania, Stradale Primosole 50, I-95121 Catania, Italy

(Received 22 February 2005; accepted 19 April 2005; published online 16 June 2005)

In this paper, the effects of ion irradiation on Schottky barriers formed on silicon carbide are discussed. After Si-ion irradiation at the near-interface region in Ti/4H-SiC contacts an increase of the Schottky barrier height from 1.05 to 1.21 eV was observed, accompanied by a lowering of the reverse leakage current. The combination of several methods allowed us to determine the physical properties of the Schottky barrier and to explain the mechanism responsible for the barrier height changes. In particular, the structural and electrical modifications of the interfacial region, both of Ti layer and SiC (i.e., different orientation of the Ti layer, irradiation-induced defects in the epilayer, dopant deactivation, and the consequent reduction of the surface electric field) are responsible for the increase of the Schottky barrier height and the reduction of the leakage current. The electrical characterization of the contacts at different temperatures also suggested that ion irradiation induced modifications in the inhomogeneous nature of the Ti Schottky barrier. © *2005 American Institute of Physics*. [DOI: 10.1063/1.1928328]

I. INTRODUCTION

The knowledge of the carrier transport mechanisms across metal/semiconductor contacts is a fundamental research topic, also having a technological relevance for a large variety of applications in the field of semiconductor electronic devices. In particular, as a consequence of the growing interest towards wide-band-gap materials for high-power and high-temperature applications, several studies on Schottky barriers on silicon carbide (SiC) were reported in the last years.[1–8] Common to these studies is the crucial need of a deep understanding of the physical properties of Schottky barriers on SiC, with the final aim to improve the contact reliability for practical devices fabrication.

Nowadays, SiC has adopted many well-consolidated processes of silicon technology, such as ion implantation, which was already used for selective material doping[9–12] and for the formation of high resistive edge terminations in SiC Schottky rectifiers.[13,14] In this way, a semiconductor technology based on SiC has been developed. Obviously, improving the SiC device processing is strictly related to the understanding of basic mechanisms such as the electrical activation of dopants, the annealing of irradiation-induced defects, etc. As a matter of fact, recent studies reported on the effects of ion irradiation on the electrical active dopant concentration in SiC.[15,16]

Interestingly, in some fields, such as the testing of radiation hardness for aerospace industry[17] and the development of particle detectors,[18] it is extremely important to correlate the effects of ion irradiation on the material properties with the modifications of the electrical characteristics of Schottky barriers.

While ion implantation has been already used in the past to tailor the Schottky barrier heights in silicon[19–24] and in other semiconductor materials,[25,26] to date the modifications of Schottky barriers on SiC, induced by ion irradiation of the near-surface region, were not object of extensive investigations.

In our preliminary study, we illustrated the effects of ion irradiation on the structure of a Ti layer as Schottky contact on 4H-SiC.[27]

Titanium was chosen in our studies because since it is one of the most widely used metals for Schottky contacts in commercial SiC devices, giving a good compromise between the forward voltage drop and the reverse current. However, the precise control of Ti/SiC Schottky barrier properties still remains a key technological issue, being the reproducibility strongly affected by the surface preparation and by the post-metallization annealing treatments. In fact, Ti mostly forms non-ideal Schottky contacts on SiC with low barrier values after metal deposition[28] and thermal treatments in the range of 673–773 K are commonly carried out to improve the rectifying properties of the barrier.[5,28,29] However, these annealings may result in the formation and the coexistence of different phases (silicides and/or carbides),[29–31] and lead to an inhomogeneous Schottky barrier, i.e., a contact characterized by the presence of a non-uniform lateral distribution of the barrier height values.

In this paper, the effects of Si-ion irradiation on Ti Schottky barriers on SiC were studied in more detail, by combining several experimental techniques. In this study, it will be shown that the increase of the Schottky barrier height after ion irradiation can be correlated to the ion-beam-induced modifications of the Ti/4H-SiC interfacial region, such as dopant deactivation and irradiation-induced defect formation. The electrical characteristics of the contacts will be also discussed in terms of the inhomogeneous nature of the Schottky barrier.

[a]Electronic mail: fabrizio.roccaforte@imm.cnr.it

II. EXPERIMENTAL DETAILS

The experiments were carried out using *n*-type (nitrogen doped) 4H-SiC (0001) epitaxial layers (4 μm thick) with a carrier concentration of $N_D = 2.4 \times 10^{16}$ cm^{-3}, grown onto an n^+ highly doped substrate.

In order to study the physical properties of the metal/SiC barrier under ion irradiation, Schottky barrier diodes were fabricated on these samples using the following procedure. First, a silicon dioxide layer, 1 μm thick, was deposited on the wafer front side by chemical-vapor deposition technique. The Ohmic contact on the wafer rear was formed by *e*-gun evaporation of a 150-nm-thick Ni film, followed by rapid thermal annealing at 1223 K in N_2 atmosphere. A device active area of 0.69×10^{-2} cm^2 was defined by opening windows on the oxide by means of optical lithography combined with oxide wet etch in a buffered HF solution. The Schottky contact was formed by sputtering a 300-nm-thick Ti film. In the same sputter run, a 3.5-μm-thick Al layer was sequentially deposited after Ti to facilitate the device bonding. A second photolithography, followed by a chemical etch, allowed to define a metal field plate over the oxide. Finally, the diodes were annealed at 723 K in Ar atmosphere for 30 min. This annealing served to improve both the rectification properties of the Ti barrier[5,28,29] and the metal stack adhesion.

The diodes were then irradiated with an 8-MeV Si^{+4} beam, at fluences ranging between 1×10^9 and 1×10^{12} ions/cm^2. The value of the ion-beam energy was chosen in order to localize the implanted ions in the proximity of the metal/SiC interface. Figure 1 schematically reports the experimental irradiation conditions of the diodes [Fig. 1(a)], as well as the depth distribution of the implanted ions [Fig. 1(b)] calculated using the TRIM code,[32] which gave a value of the projected ion range through the Al/Ti/4H-SiC of 4.1 μm.

The electrical characterization of the Ti/4H-SiC Schottky barrier was performed by current–voltage (*I–V*) measurements of the diodes at different temperatures using a Keithley 2410 source meter unit. The structural analysis of the metal/SiC interfacial region was carried out by transmission electron microscopy (TEM), performed on a 200-kV JEM 2010 JEOL microscope equipped with a Gatan imaging filtering (GIF) used for energy filtering TEM (EFTEM).

Scanning capacitance microscopy (SCM) was used to determine the doping level of the SiC epilayer at the near-interface region which was interested by the ion-irradiation effects. SCM measurements were performed with a Digital Dimension 3100 atomic force microscope, equipped with the SCM head. The direct inversion method has been applied to convert the row data into concentration profiles.

The formation of ion-irradiation-induced defects was monitored by deep-level transient spectroscopy (DLTS), performed with a Bio-Rad 4600 equipment. DLTS measurements were carried out applying reverse bias values of −10 or −1 V and filling pulses between −0.5 and +0.5 V in order to monitor a wide bulk depth. With the same equipment, capacitance–voltage (*C–V*) curves were acquired at different temperatures both for the unirradiated and the irradiated samples.

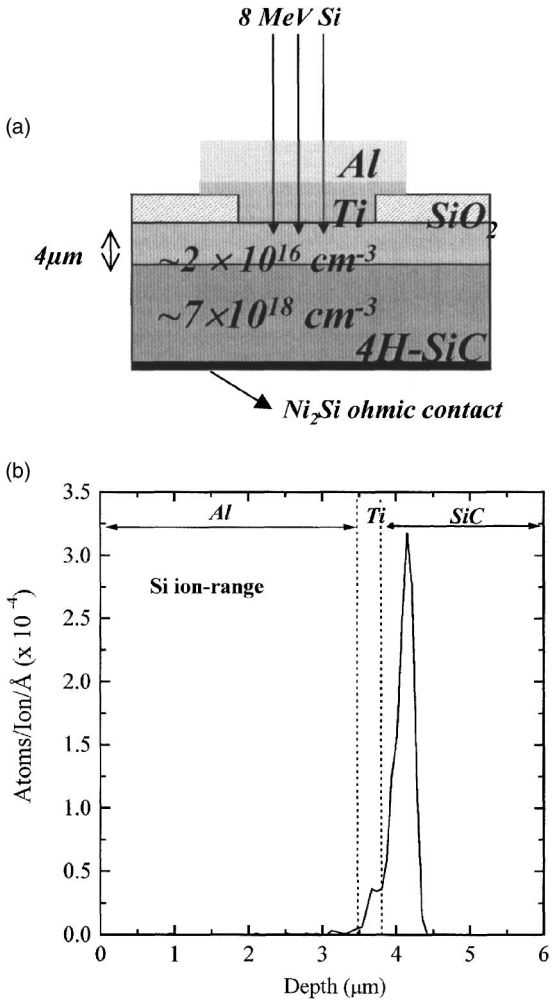

FIG. 1. (a) Schematic of Ti/4H-SiC Schottky diodes and experimental conditions of ion irradiation; (b) TRIM simulation of the concentration profile of 8-MeV Si ions.

III. EXPERIMENTAL RESULTS

A. Electrical characterization of the Schottky barrier

The forward and reverse *I–V* characteristics of the Ti/4H-SiC Schottky diodes before and after irradiation at the different ion fluences are reported in a semilogarithmic plot in Figs. 2(a) and 2(b), respectively.

According to the thermoionic emission theory,[33] the current *I* flowing through the contact under the application of a bias *V* is given by the following expression:

$$I = SA^{**}T^2 e^{-q\Phi_B/kT}\left[e^{q(V-IR_s)/nk_BT} - 1\right] = I_S\left[e^{q(V-IR_s)/nk_BT} - 1\right], \quad (1)$$

where *S* is the contact area, Φ_B is the Schottky barrier height, *n* is the ideality factor, A^{**} is the Richardson constant, R_s is the diode series resistance, *q* is the electron charge, k_B is the Boltzmann constant, and *T* is the absolute temperature.

From the *I–V* characteristics under forward bias [Fig. 2(a)], a fit of the linear portion of semilogarithmic plot, i.e., where $V > 3k_BT/q$ and the series resistance is negligible ($IR_s \ll V$), allowed us to determine the values of the Schottky barrier height Φ_B and of the ideality factor *n*. For this calcu-

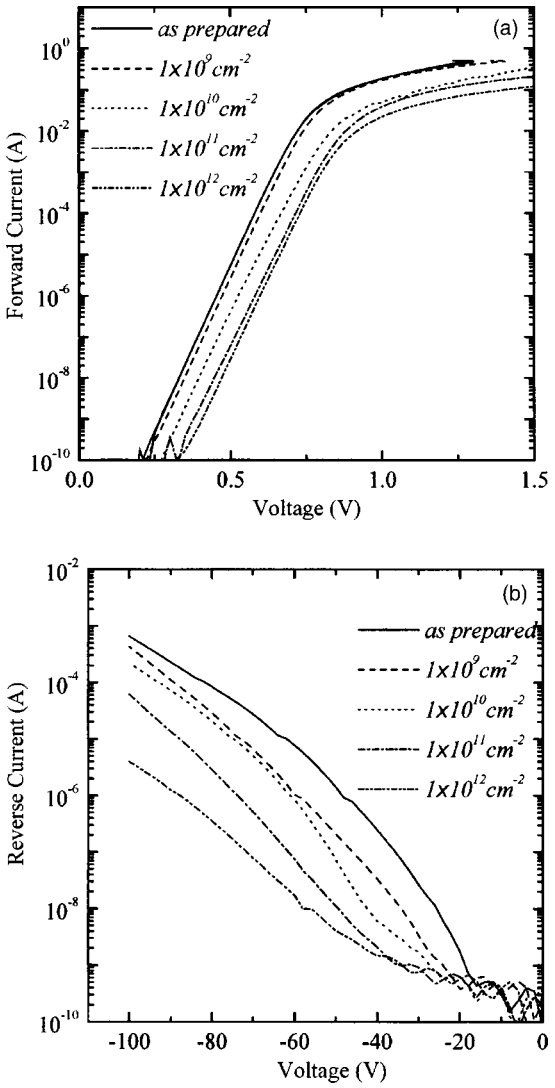

FIG. 2. (a) Forward and (b) reverse *I–V* characteristics of the Ti/4H-SiC Schottky diodes after preparation and after irradiation with 8-MeV Si ions at different fluence between 1×10^{9} and 1×10^{12} ions/cm^2.

lation, the theoretical value of the Richardson constant $A^{**}=146$ A/cm^2 K^2 for 4H-SiC given in Ref. 34 was used.

In the as-prepared (unirradiated) contact, a Schottky barrier height $\Phi_B=1.05$ eV and an ideality factor $n=1.08$ were determined. The value of Φ_B is lower than that expected for an ideal optimized Ti/4H-SiC contact (1.27 eV),[7] thus indicating that, as in the case of other metals,[6] the surface preparation prior to metal deposition plays a fundamental role also in the formation of Ti Schottky contacts on SiC.

On the other hand, under reverse bias, the values of the leakage current were 2.4×10^{-7} A at -40 V and 6.5×10^{-4} A at -100 V, as can be seen in Fig. 2(b).

After irradiation of the samples, an increase of the value of the Schottky barrier is observed with increasing ion fluence, as shown in Fig. 2(a) by the shift towards higher biases of the *I–V* curves. The increase of Φ_B is connected to a decrease of the leakage current, as clearly visible in Fig. 2(b). In particular, after irradiation at a fluence of 1×10^{12} ions/cm^2, a value of $\Phi_B=1.21$ eV was found, without any substantial change of the ideality factor *n*. Moreover, at the same irradiation flunce, a significant decrease of the leakage current was observed (1.5×10^{-9} A at -40 V and 4×10^{-6} A at -100 V). It is important to point out that a further post-irradiation annealing at 723 K did not lead to a variation of the electrical characteristics of the contacts. Post-annealing treatments at higher temperatures were not performed in order to avoid a barrier degradation due to solid-state reactions of Ti with SiC.

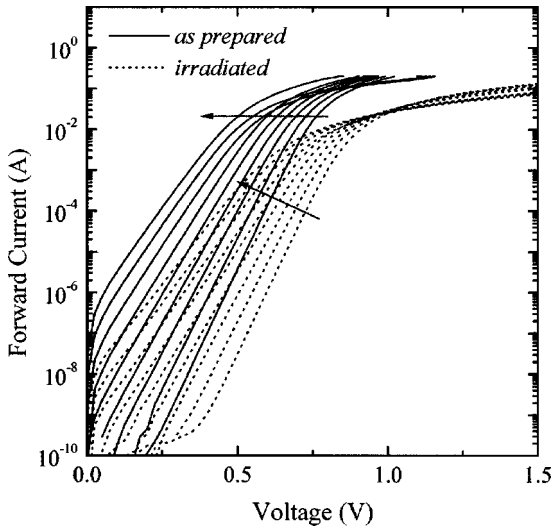

FIG. 3. Forward *I–V* characteristics of unirradiated (as-prepared) and irradiated (at the dose of 1×10^{12} ions/cm^2) Ti/4H-SiC Schottky diodes at different temperatures between 300 and 500 K. The arrows indicate the direction of increasing temperatures.

Further physical information on the nature of the Schottky barrier could be acquired by the electrical characterization of the contacts performed as a function of temperature.

Figure 3 shows the forward *I–V* characteristics of the as-prepared (unirradiated) diode and of the diode implanted at the highest fluence, acquired at temperatures between 300 and 500 K.

At low forward bias values (i.e., up to 0.75 V), the *I–V* curves exhibit a linear behavior with the current increasing by increasing temperatures, as expected when the current transport is ruled by the thermoionic emission mechanism.

As can be seen from Eq. (1), the saturation current I_s can be written as

$$I_s = SA^{**}T^2 e^{-q\Phi_B/kT}. \tag{2}$$

The values of I_s at the different temperatures were determined by the linear fit of the *I–V* curves.

Then, by reporting the $\ln(I_s/T^2)$ as a function of $1/T$, in the so-called Richardson plot, by the *slope* and the *intercept* of the fit it is possible to determine the values of the effective Schottky barrier $\Phi_B(=-k/q\times \textit{fit-slope})$ and of the product $SA^{**}(=e^{\text{intercept}})$, respectively. The advantage of this method consists in the fact that the extracted value of the Schottky barrier height is independent of the exact knowledge of the "effective area" of the contact. This latter is an important concept, since in "real" metal/semiconductor contacts the effective area taking part to the current conduction can be significantly different from the geometric diode area.

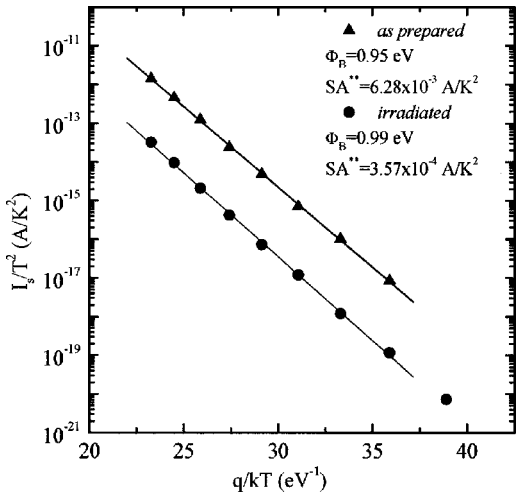

FIG. 4. Richardson's plot for the as-prepared contact and for the contact irradiated at the dose of 1×10^{12} ions/cm^2.

From the slopes of the Richardson plots, shown in Fig. 4, a value of $\Phi_B=0.95$ eV for the as-prepared contact and a value of 0.99 eV for the irradiated contact were extracted. The values of Φ_B determined by the Richardson plot are quite lower than those determined by the forward *I–V* characteristics at room temperature reported in Fig. 2(a). In particular, the value of the product SA^{**} for the unirradiated contact (6.28×10^{-3} A/K^2) was higher than that found in the irradiated contact (3.57×10^{-4} A/K^2). From these values, the experimental Richardson constant can be determined using the value of the contact's area *S*. In both cases, a strong deviation of the experimental values of the Richardson constant from its theoretical value of 146 A/cm^2 K^2 ($A^{**}=9.1\times10^{-1}$ A/cm^2 K^2 in the unirradiated and 5.1×10^{-2} A/cm^2 K^2 in the irradiated barrier) was found.

The nature of the metal/SiC barrier could be better understood by studying the temperature dependence of the calculated Schottky barrier height Φ_B and of the ideality factor *n*. As can be clearly seen in Fig. 5(a), both *n* and Φ_B exhibit a dependence on the temperature *T*. In particular, by increasing the temperature, while the ideality factor decreases approaching the unity at high temperatures (especially in the unirradiated contact, where $n=1.02$ at 500 K), an increase of the Schottky barrier height with respect to the value measured at room temperature is observed.

In the unirradiated contact the ideality factor decreases from $n=1.08$ at 300 K to $n=1.02$ at 500 K, while Φ_B increases from 1.08 to 1.17 eV. On the other hand, in the irradiated sample, while only a slight decrease, below 2%, of the ideality factor occurs ($n=1.09$ at 300 K and $n=1.07$ at 500 K), a significant variation of Φ_B from 1.21 to 1.34 eV is observed.

The dependence on the temperature of the physical parameters *n* and Φ_B, together with the different values of the product SA^{**} found in the contact before and after irradiation, indicates the presence of "inhomogeneous" Schottky barriers. An inhomogeneous Schottky barrier can be seen as formed by a distribution of low barrier "patches" embedded in a uniform high barrier background.[35,36] This picture was assumed by Im *et al.*[37] to describe the experimental behavior

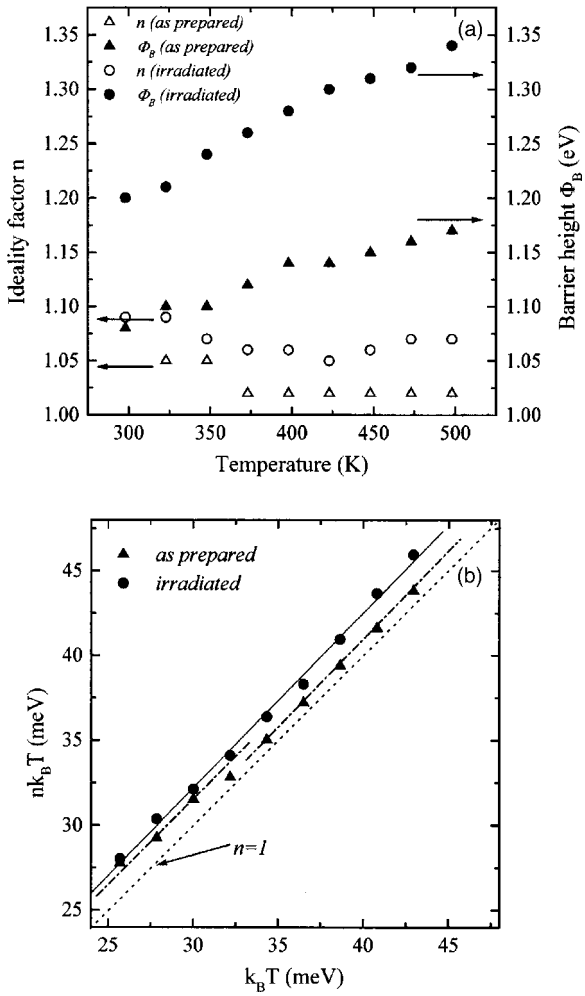

FIG. 5. (a) Barrier height Φ_B and ideality factor *n* as a function of the temperature; (b) plot of nk_BT vs k_BT; the dashed straight line is the ideal case $n=1$. These plots are reported both for the unirradiated (as-prepared) and for the irradiated Ti/4H-SiC contacts.

of non-ideal inhomogeneous Pd/6H-SiC barriers, demonstrating the presence of a nanometer scale distribution of the barrier heights by means of ballistic electron emission microscopy.[38]

In the presence of an inhomogeneous barrier, by increasing temperature, the current flow through the high barrier regions becomes dominant, i.e., the carriers can overcome the highest barrier nearly by pure thermoionic mechanism. Therefore, the ideality factor is very close to 1 and a high value of Φ_B is measured. On the other hand, at low temperatures, electrons have sufficient energy only to pass the lower barrier patches, which leads to a deviation from the ideal behavior and to lower values of Φ_B.

However, it is worth noting that the tendency to approach the ideal behavior at high temperature is more evident in the unirradiated contact. This latter conclusion is confirmed by the data reported in Fig. 5(b), which shows the plot of nk_BT as a function of k_BT both for the as-prepared and the irradiated contacts. The dashed line, also shown in the figure, indicated the ideal behavior ($n=1$). In the unirradiated contact, while the experimental points at low temperatures lie parallel to the line of the ideal behavior, a "more ideal" behavior ($n=1.02$) is observed at high temperatures. This be-

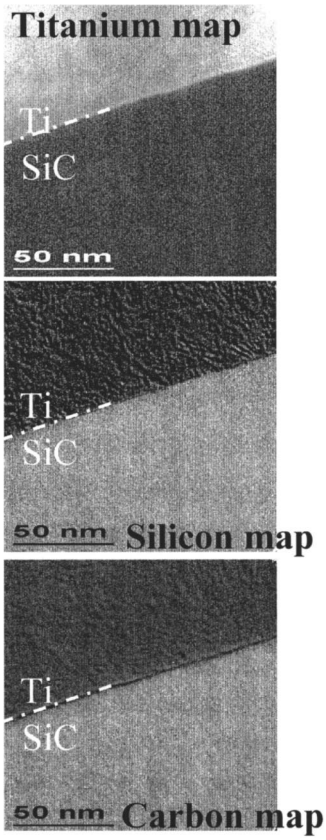

FIG. 6. EFTEM maps of Ti, Si, and C taken at the near-interface region of a Ti/4H-SiC Schottky contact after irradiation with 8-MeV Si ions at a fluence of 1×10^{12} ions/cm^2. The bright contrast indicate the presence of the element. The position of the metal/SiC interface is also indicated.

havior is similar to what observed by Aboelfotoh[39] in inhomogeneous barriers on silicon. On the other hand, in the irradiated contact, the experimental data are almost parallel to the straight line of the ideal case in the entire temperature range. As pointed out by Sullivan *et al.*,[35] this kind of behavior of an inhomogeneous barrier indicates that the ideality factor can be expressed as $n\sim1+T_0/T$ and is commonly referred as the "T_0 anomaly." From a linear fit of the data, for the irradiated Schottky barrier, a value of $T_0=36$ K could be determined. Hence, all these findings suggest that a different "degree of inhomogeneity" exists between the unirradiated and the irradiated contact.

B. Structural analysis of the interface

The chemical analysis of the irradiated metal/SiC interfacial region was performed by means of EFTEM. This technique[40] allows one to determine the elemental chemical composition of a sample with the spatial resolution of TEM, by subjecting the transmitted electron beam to an energy filtering process after the interaction with the specimens present in the matrix. Therefore, in the EFTEM maps, shown in Fig. 6, a bright contrast indicates the presence of the element. The position of the Ti/SiC interface is also marked in the figure as a reference. The sample reported in the figure was implanted to a fluence of 1×10^{12} ions/cm^2.

The maps of the elements reveal the presence of Ti only inside the metal film, i.e., neither the annealing at 723 K nor

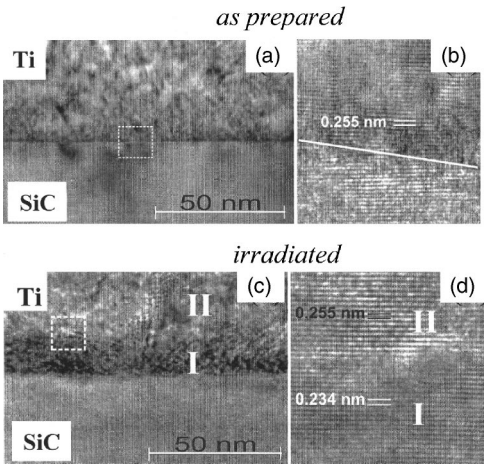

FIG. 7. [(a) and (c)] Cross-section TEM micrograph of as-prepared and irradiated (1×10^{12} ions/cm^2) Ti/4H-SiC contacts. [(b) and (d)] High-resolution TEM images of the marked regions, showing the different orientations of Ti in the regions I and II. The line in (b) indicates the interface Ti/SiC (the epitaxial layer is 8° off axis).

the following ion irradiation induced a solid-state reaction or ion mixing of Ti with the SiC substrate. Hence the meal/SiC interface remained chemically unchanged, without the formation of silicides or carbides.

On the other hand, the TEM analysis indicates that a structural modification of the Ti layer has occurred after irradiation. Figure 7 shows the TEM images in cross section of the Ti/4H-SiC interfacial region, both for the as-prepared sample (top) and for the sample irradiated at the fluence of 1×10^{12} ions/cm^2 (bottom). The low magnification TEM image of the unirradiated contact, Fig. 7(a), shows a sharp metal/SiC interface, along with a uniform contrast inside the Ti metal layer. High-resolution TEM taken in this interface [Fig. 7(b)] demonstrated that the Ti film is epitaxially oriented onto the SiC substrate, with the orientation Ti$(10\bar{1}0)$ or Ti$(0\bar{1}10)$ ∥ SiC(0001). A different scenario appears in the irradiated sample where, while the planarity of the interface is almost completely preserved, two regions with a different contrast inside the Ti metal layer [indicated with I and II in Fig. 7(c)] can be distinguished. The thin layer with the dark contrast (1), visible in the proximity of the interface with the SiC substrate, was continuous over the whole interfacial region with an average thickness of about 8 nm. Although the EFTEM analysis on the same sample (shown in Fig. 6) did not reveal any compositional change of the interface after irradiation, the high-resolution TEM image shows that a modification of the Ti layer structure has occurred after irradiation. The high-resolution image taken between the regions I and II is shown in Fig. 7(d). Interestingly, from the analysis of the high-resolution TEM a different crystallographic orientation of the two regions of the Ti layer was determined. Indeed, the thin layer (1) located in the proximity of the interface had the same crystallographic orientation of the SiC substrate with the Ti(0001) ∥ SiC(0001) and this layer was almost continuous along the interface with SiC. On the other hand, the remaining upper part (II) of the Ti layer had a different crystallographic orientation, i.e., the Ti$(10\bar{1}0)$ or Ti$(0\bar{1}10)$ ∥ SiC(0001). The distance between two planes of

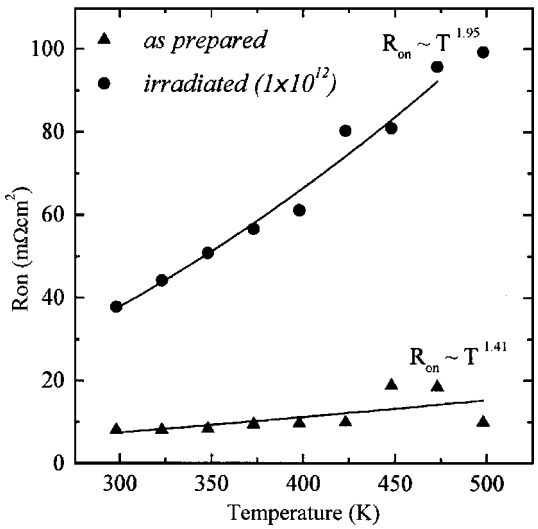

FIG. 8. Specific on-resistance R_{on} as a function of temperature T. In the as-prepared contact $R_{on} \propto T^{1.41}$ while in the irradiated contact $R_{on} \propto T^{1.95}$.

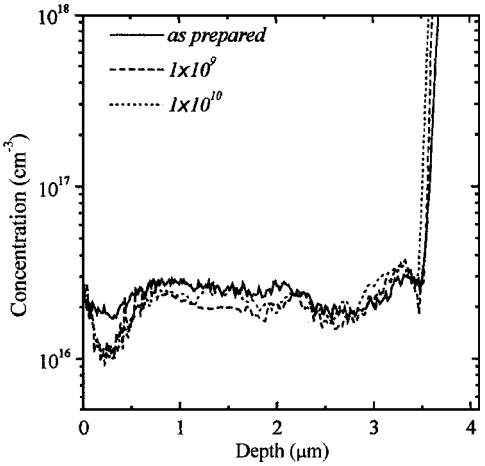

FIG. 9. Carrier concentration profile determined by SCM for the as-prepared sample and for the samples irradiated at the ion fluences of 1×10^9 and 1×10^{10} ions/cm^2. The dopant deactivation is visible in the irradiated samples.

the Ti aligned with the SiC surface varies from 0.234 nm of the Ti(0002) close to the interface (1) to 0.255 nm of the Ti($10\bar{1}0$) or Ti($01\bar{1}0$) in the remaining upper part of the film (II). It is important to point out that the presence of this continuous thin layer of Ti at the interface with the orientation Ti(0001) ∥ SiC(0001) was not detected by the TEM analyses performed on the unirradiated sample, where instead only the Ti($10\bar{1}0$) growth direction could be observed.

C. Ion-irradiation-induced modifications on SiC material

Beyond the structural changes of the Ti film observed by the high-resolution TEM analysis, ion irradiation also induces modifications in the SiC substrate, in terms of deep defect creation and dopant deactivation, which in turn strongly contribute to the experimentally observed barrier height changes.

The forward *I–V* characteristics performed as a function of the temperature *T*, previously shown in Fig. 3, indicate that at forward biases higher than 0.75 V, a decrease of the current by increasing the temperature occurs. In this region, the electrical behavior of the diodes is dominated by the series resistance R_s. Hence, from the experimental *I–V* data, the specific on-resistance $R_{on}=R_sS$ (mΩ cm^2) could be determined by using the Nordes method.[41] In Fig. 8, R_{on} is reported as a function of the temperature *T* for both the as-prepared and the irradiated diodes. Two comments must be done on these results.

First, the results clearly indicate an increase of the R_{on} value in the irradiated sample in all the measured temperature range. In particular, at room temperature, the specific on-resistance increased from 8 to 37 mΩ cm^2 after irradiation, thus indicating that the ion-irradiation-induced damage in the epilayer modifies the material properties, leading to an increase of the semiconductor resistivity. The increase of the resistance can be due to a decrease of the active carrier concentration N_D and/or to a decrease of the mobility μ. Secondly, a stronger temperature dependence of R_{on} is observed in the irradiated material. In fact, a dependence of the type $R_{on} \sim T^{1.41}$ in the unirradiated contact and of the type $R_{on} \sim T^{1.95}$ in the irradiated contact was found. This latter indicates that the carrier transport mechanism in SiC was affected by ion irradiation. In particular, the presence of defects in the epilayer after irradiation determines a different temperature dependence of the electron drift mobility μ,[42,43] which, in turn, results in a different temperature coefficient of R_{on}.

Also the concentration of active dopant at the near-interface region was affected by ion irradiation. The electrically active dopant concentration profiles of the as-prepared diode and of the diodes irradiated at 1×10^9 ions/cm^2 and at 1×10^{10} ions/cm^2 were determined by the SCM analysis as described in detail in Ref. 44 and are reported in Fig. 9. At the near-interface region, i.e., the region that was interested by ion irradiation, a decrease in the carrier concentration, of about a factor of 2 with respect to the initial value, can be observed. This latter indicates that ion irradiation produced a deactivation, or energy-level compensation, of the nitrogen dopant species in the proximity of the Ti/SiC interface. For the samples irradiated at the higher fluences (1×10^{11} and 1×10^{12} ions/cm^2), the electrical deactivation at the near-interface region was certainly much higher than a factor of 2. However, at these fluences quantification of the deactivation by the SCM profiles was not possible, being the electrically active nitrogen concentration below the sensitivity limit of the technique.

The *C–V* characteristics of the contacts were also very sensitive to the ion-irradiation effects. In Fig. 10 the $1/C^2$ is reported as a function of the reverse bias *V* at different temperatures for the unirradiated (solid lines) and for the irradiated contact (1×10^{12} ions/cm^2, dashed lines).

In the unirradiated Ti/4H-SiC Schottky contact, a linear $1/C^2$ curve is observed, almost regardless of the temperature. As well known, the slope of the line provides the free-carrier concentration value, which at 300 K is of about 1×10^{16} cm^{-3}, slightly lower than the nominal value, for the epi-SiC wafers used, of 2.4×10^{16} cm^{-3}. Moreover, the inter-

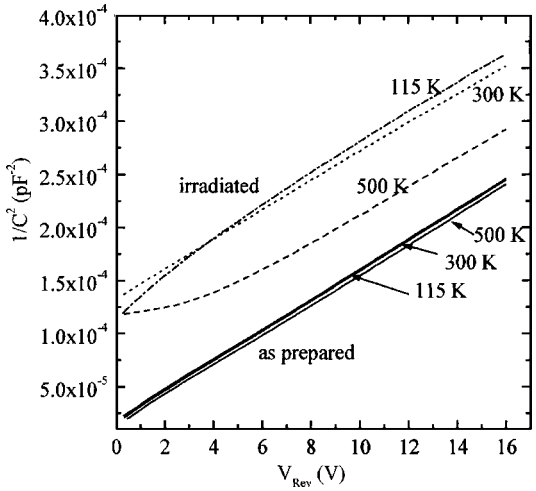

FIG. 10. $1/C^2$ vs V plots taken at three different temperatures for the unirradiated (as-prepared) and irradiated Ti/4H-SiC Schottky contacts.

cept with the abscissa of the linear fit of the data provides the built-in potential, $V_{bi}=1.23$ eV at room temperature. From such value it was possible to determine the barrier height value of $\Phi_B=1.40$ eV. The value obtained with the C–V measurements is much higher that the value obtained from the I–V measurements. The difference in the two results is due to the different approach used for the measure. In particular, a C–V measurement is not a "transport technique" since it does not involve free-carrier transport. Furthermore, in the case of an inhomogeneous Schottky barrier, this technique is more sensitive to the high barrier regions while I–V measurements are more affected by the low barrier patches.[45] In the same figure are also plotted the C–V curves taken at different temperatures, 115 and 500 K. The free-carrier concentration is not affected by the temperature in the measured range, as can be deduced by the fact that all the lines have the same slope. A small variation is observed in the built-in potential (the lines are slightly shifted).

On the other hand, the irradiated diodes exhibited an anomalous bending of the $1/C^2$ curves, more evident at low reverse biases, and a strong dependence of the capacitance itself on the temperature. In particular, after irradiation, the $1/C^2$ data at room temperature show a constant free-carrier concentration, but its value is one order of magnitude higher than that of the unirradiated sample. Moreover, the barrier height obtained from these data is strongly affected by the deep levels present in the sample. In fact, in the presence of a high concentration of deep levels anomalous $1/C^2$ curves are obtained and a simple interpretation of data is rather difficult. Hence, it was not possible to determine meaningful values of the Schottky barrier height and semiconductor doping concentration. A further confirmation of the presence of a high damage concentration is obtained by the $1/C^2$ curve at 500 K. It is not a straight line, as expected for a Schottky barrier, but a strong bend is visible. It can be inferred that when deep levels are present in the material band gap, the capacitance behaves as shown in Fig. 10,[46] since both the free-carrier concentration and the depletion layer depend on the ionized deep trap concentration.

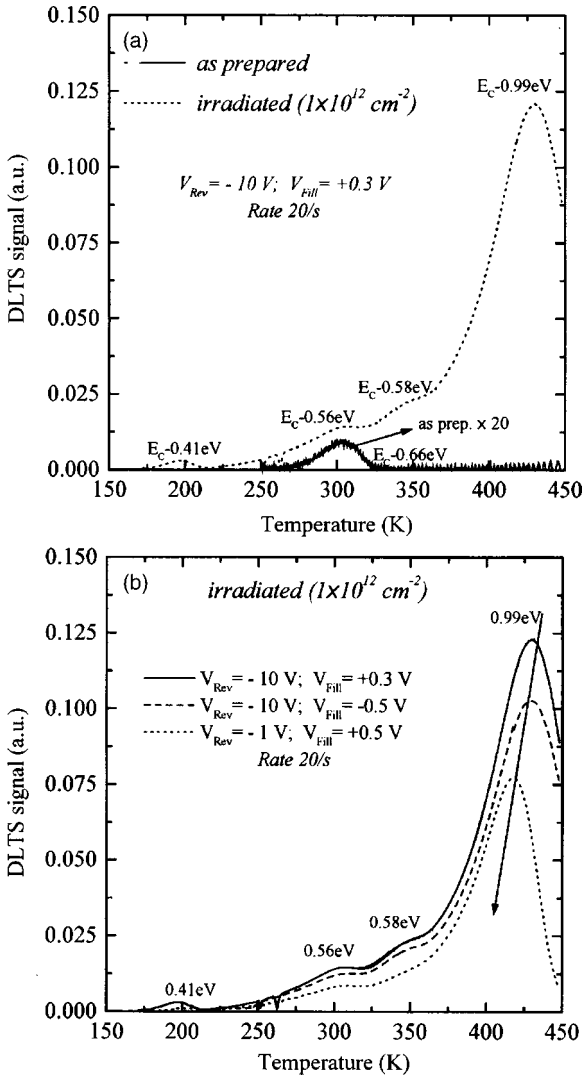

FIG. 11. (a) DLTS spectra of the as-prepared and irradiated materials. (b) DLTS spectra of the sample after irradiation at 1×10^{12} ions/cm^2 acquired at different V_{fill} values. The decrease of the DLTS signal indicates a decrease of the defects concentration by moving from the interface to the bulk.

In order to investigate the presence of ion-irradiation-induced defects in the SiC material, the DLTS analysis of the samples was performed. These measurements are summarized in Fig. 11(a), which shows the DLTS signal for the unirradiated and for the irradiated contacts. The as-prepared sample (solid line) shows two energy levels in the gap, barely visible in the figure due to the scale used to plot the deep levels of the implanted sample. The levels lie at $E_C-0.16$ eV and $E_C-0.66$ eV, with a maximal uncertainty of 0.02. The first level exhibits a trap concentration of 4.7×10^{12} cm^{-3} close to the measurement sensitivity limit (9×10^{11} cm^{-2}). The other deep center can be associated with the well-known Z_1/Z_2 level, always detectable in the as-prepared samples,[47] and present in a concentration of 5.7×10^{12} cm^{-3}.

After the implantation the deep level concentration is strongly increased. Evidently, irradiation leads to the formation of defect centers in SiC as the implanted sample (dashed line) exhibits four different trap energy levels located at $E_C-0.99$ eV, $E_C-0.58$ eV, $E_C-0.56$ eV, and $E_C-0.41$ eV. The

uncertainty on these values is ~0.02 eV. Also in these samples the low-energy level is present, but its concentration is unaffected by the implantation process, hence it will not be further discussed. The first mentioned level at $E_C-0.99$ eV has a concentration above 2.5×10^{15} cm^{-3} and significantly affects the free-carrier concentration, as already observed in the previously described *C–V* measurements. Hence, the exact concentration value of this level cannot be inferred by DLTS. This level can be associated with the irradiation-induced RD_3 center, whose microscopic nature is not well identified yet.[48] The other levels are present in the concentration of 7.4×10^{14}, 4.4×10^{14}, 7.1×10^{13} cm^{-3}, respectively. These levels were not present before irradiation, as confirmed by the DLTS spectrum of the as-prepared sample.

Clearly, the DLTS results show that ion irradiation led to modifications in the SiC material, by inducing the formation of deep levels in the SiC band gap. In particular, the presence of energy trap levels in the irradiated material is responsible for the behavior observed in the *C–V* curves. In Fig. 11(b) the DLTS spectra acquired at different values of filling bias (V_{fill}) are reported. The differences in the curve heights clearly indicate that the defect concentration decreases by moving from the interface to the bulk. This latter is consistent with a profile of defects decorating the depth distribution of the implanted ions below the Ti/SiC interface.

IV. DISCUSSION

The combination of different analytical techniques reported in this work enabled us to draw a possible scenario explaining the ion-irradiation-induced modifications of the electrical properties of the Ti Schottky barrier on 4H-SiC.

It must be reminded that different factors determine the value of the Schottky barrier height at a metal/SiC interface. The difference between the metal and the semiconductor work function in SiC is mainly responsible for the dependence of Φ_B on the barrier metal.[1,2] However, the value of the barrier is strongly affected by the presence of interface states, determined by the interface intrinsic properties and/or by the surface preparation method before metal deposition.[49] Finally, as known by other semiconductor materials, also the presence of an insulating interfacial layer[50] or local variations of the electric field at the semiconductor surface[21] can affect the electrical properties of the Schottky contacts.

Therefore, a first consideration concerning the modification of the Ti structure must be done. As observed by the TEM analysis, ion irradiation modifies the orientation of the Ti film near the interface, thus being a consequence of the ion energy deposition at the interfacial depth. Obviously, since the Schottky barrier height depends on the metal/semiconductor interface, i.e., on the metal in intimate contact with the semiconductor, and no reaction and/or mixing of Ti with SiC could be experimentally observed by the EFTEM analysis, the increase of Φ_B from 1.05 to 1.21 eV after ion irradiation can be partially ascribed to the structural changes of the Ti layer. Similarly, also in silicon a change in the orientation of a silicide phase leads to different values of the Schottky barrier height.[51]

However, more significant are the modifications of the SiC properties induced by ion irradiation at the near-interface region. As inferred by the DLTS analysis, these modifications are essentially due to the formation of ion-irradiation-induced defects, which in turn result into an increase of the temperature coefficient of the mobility ($\mu\propto T^{-1.41}$ before irradiation and $\mu\propto T^{-1.95}$ after irradiation) and a deactivation of the nitrogen dopant as observed by SCM. Accordingly, Åberg *et al.*[15] also showed that ion-irradiation-induced point defects in SiC can interact electrically with nitrogen, leading to its deactivation and to the consequent reduction of the free-carrier concentration. Then, since the *barrier thickness* depends on the electrical active doping N_D through the depletion width ($\propto N_D^{-1/2}$), in our case, a dopant deactivation at the Ti/SiC near-interface region determines an increase of the Schottky barrier thickness, which contributes to the decrease of the leakage current in reverse bias.

As a consequence of the dopant deactivation observed after irradiation, a modification of the potential and electric-field distribution occurs at the near-interface region, which can justify the increase of the barrier height.

In particular, assuming for simplicity that the irradiation induced a deactivation of the dopant over a uniform thickness *d*, the potential and electric-field distribution can be determined by solving the Poisson equation, like suggested by Wu in silicon in the presence of a highly doped surface layer.[52]

In a simple unidimensional case, the integration of the Poisson equation leads to a maximum electric field at the interface given by

$$E_{\max}=-\frac{q}{\varepsilon_{\text{SiC}}}(N_{D0}-N_{D1})d+\left(\frac{2qN_{D0}}{\varepsilon_{\text{SiC}}}\right)^{1/2}\times\left[V_{\text{ht}}-\frac{kT}{q}+\frac{q}{2\varepsilon_{\text{SiC}}}(N_{D0}-N_{D1})d^2\right]^{1/2},\tag{3}$$

where ε_{SiC} is the permittivity of the material, N_{D1} is the doping concentration at the near-interface region, and N_{D0} is the epilayer doping (i.e., $N_{D1}<N_{D0}$ in the case of deactivation).

Clearly, the maximum electric field at the metal/SiC interface is reduced by ion irradiation, this reduction depending on the deactivation $(N_{D0}-N_{D1})$ and on the modified thickness *d*. In particular, if $d=0$ or $N_{D1}=0$ (i.e., in the absence of deactivation) the expression (3) reduces to the well-known form of the maximum electric field for the Schottky contacts.

According to the interpretation given in Ref. 52, because of the dependence of the image force lowering of the barrier on the square root of the maximum electric field,

$$\Delta\Phi_B=\left(\frac{qE_{\max}}{4\pi\varepsilon_{\text{SiC}}}\right)^{1/2},\tag{4}$$

a decrease of the maximum electric field at the interface determines an increase of the Schottky barrier height.

Although the increase of the Schottky barrier is consistent with the reduced electric field at the surface, this approach is not able to quantitatively explain the experimentally observed increase of Φ_B (i.e., 0.16 eV after irradiation at 1×10^{12} ions/cm^{-2} with respect to the as-prepared

sample). Hence, it can be argued that the modifications of material properties occurred after irradiation also play a role in the barrier height increase. Indeed, it was reported that the presence of charged deep levels in the gap can determine an increase of the barrier height.[45]

Finally, it is important to point out that both the unirradiated and the irradiated Schottky contacts exhibited the typical features of a inhomogeneous barriers.

However, the electrical characterization as a function of temperature suggested that the modifications occurred in the SiC substrate resulted into a different degree of inhomogeneity in the two cases, manifesting itself by a different dependence of n and Φ_B on the temperature and by different experimental values of the Richardson constant.

V. CONCLUSIONS

In conclusion, strong modifications of the Schottky barriers on 4H-SiC are obtained by ion irradiation. In particular, in this work it has been observed that ion irradiation of the near-interface region of Ti/4H-SiC Schottky contacts with 8-MeV Si to a dose up to 1×10^{12} cm^{-2} resulted into an increase of the Schottky barrier height and a decrease of the reverse leakage current by nearly two orders of magnitude.

A combination of several experimental techniques allowed us to clarify the physical mechanism responsible for the changes of the electrical properties of the Ti/4H-SiC barrier after irradiation. Along with the structural modifications of the Ti layer, significant changes of the electrical properties of the SiC epilayer were detected in the irradiated samples. In fact, the presence of irradiation-induced defects in the SiC epilayer modified the carrier transport properties (as deduced by the temperature dependence of the drift mobility) and led to a dopant deactivation, most probably by the passivation of nitrogen dopant. As a consequence of the deactivation, a reduction of the electric field at the surface occurs, which can lead to the increase of the Schottky barrier height value.

A different temperature behavior of the electrical characteristics also indicated that ion irradiation modified the inhomogeneous nature of the Ti/4H-SiC Schottky barrier.

Beyond representing a further improvement in understanding the Ti/SiC Schottky barrier, with an optimal choice of the irradiation parameters these results could find useful applications in the control of the Schottky barriers on SiC devices.

ACKNOWLEDGMENTS

The authors are grateful to A. La Magna for fruitful discussions. They also thank S. Di Franco for his support in the fabrication of the Schottky diodes and A. Marino for his assistance during ion irradiation.

[1]L. M. Porter and R. F. Davis, Mater. Sci. Eng., B **34**, 83 (1995).
[2]M. J. Bozack, Phys. Status Solidi B **202**, 549 (1997).
[3]B. J. Skromme, E. Luckowski, K. Moore, M. Bhatnagar, C. E. Weitzel, T. Gehoski, and D. Ganser, J. Electron. Mater. **29**, 376 (2000).
[4]C. Raynaud, K. Isoird, M. Lazar, C. M. Johnson, and N. Wright, J. Appl. Phys. **91**, 9841 (2002).
[5]M. O. Aboelfotoh, C. Fröjdh, and C. S. Petersson, Phys. Rev. B **67**, 075312 (2003).
[6]F. Roccaforte, F. La Via, V. Raineri, L. Calcagno, P. Musumeci, and G. G. Condorelli, Appl. Phys. A **77**, 827 (2003).
[7]F. Roccaforte, F. La Via, V. Raineri, R. Pierobon, and E. Zanoni, J. Appl. Phys. **93**, 9137 (2003).
[8]T. Teraji and S. Hara, Phys. Rev. B **70**, 035312 (2004).
[9]K. Wongchotigul, in *Properties of Silicon Carbide*, edited by G. L. Harris (INSPEC, IEE, London, 1995), pp. 157–161.
[10]D. Dwight, M. V. Rao, O. W. Holland, G. Kelner, P. H. Chi, J. Kretchmer, and M. Ghezzo, J. Appl. Phys. **82**, 5327 (1997).
[11]N. S. Saks, S.-H. Ryu, and A. V. Suvorov, Appl. Phys. Lett. **81**, 4958 (2002).
[12]M. Lazar, C. Raynaud, D. Planson, J.-P. Chante, M.-L. Locatelli, L. Ottaviani, and Ph. Godignon, J. Appl. Phys. **94**, 2992 (2003).
[13]A. P. Knights *et al.*, J. Appl. Phys. **87**, 3973 (2000).
[14]K. J. Schoen, J. M. Woodall, J. A. Cooper, and M. R. Melloch, IEEE Trans. Electron Devices **45**, 1595 (1998).
[15]D. Åberg, H. Allen, P. Pellegrino, and B. G. Svensson, Appl. Phys. Lett. **78**, 2908 (2001).
[16]H. Matsuura, K. Aso, S. Kagamihara, H. Iwata, T. Ishida, and K. Nishikawa, Appl. Phys. Lett. **83**, 4981 (2003).
[17]S. Nigam *et al.*, Appl. Phys. Lett. **81**, 2385 (2002).
[18]F. Nava, E. Vittone, P. Vanni, G. Verzellesi, P. G. Fuochi, C. Lanzieri, and M. Glaser, Nucl. Instrum. Methods Phys. Res. A **505**, 645 (2003).
[19]J. M. Shannon, Appl. Phys. Lett. **24**, 369 (1974).
[20]J. M. Shannon, Appl. Phys. Lett. **25**, 75 (1974).
[21]Y. P. Pai and H. C. Lin, Solid-State Electron. **24**, 929 (1981).
[22]S. Ashok, H. Kräutle, and H. Beneking, Appl. Phys. Lett. **45**, 431 (1984).
[23]R. Singh and S. Ashok, Appl. Phys. Lett. **47**, 426 (1985).
[24]J. S. Kim, H. H. Choi, S. H. Son, and S. Y. Choi, Appl. Phys. Lett. **79**, 860 (2001).
[25]J. Osvald, J. Appl. Phys. **90**, 6205 (2001).
[26]M. J. Legodi, F. D. Auret, S. A. Goodman, and J. B. Malherbe, Nucl. Instrum. Methods Phys. Res. B **148**, 441 (1998).
[27]F. Roccaforte, C. Bongiorno, F. La Via, and V. Raineri, Appl. Phys. Lett. **85**, 6152 (2004).
[28]J. R. Waldrop and R. W. Grant, Appl. Phys. Lett. **62**, 2685 (1993).
[29]D. Defives, O. Noblanc, C. Dua, C. Brylinski, M. Barthula, V. Aubry-Fortuna, and F. Meyer, IEEE Trans. Electron Devices **46**, 449 (1999).
[30]D. Defives, O. Durand, F. Wyezisk, J. Oliver, O. Noblank, and C. Brylinski, Mater. Sci. Forum **338–342**, 411 (2000).
[31]F. La Via, F. Roccaforte, A. Makhtari, V. Raineri, P. Musumeci, and L. Calcagno, Microelectron. Eng. **60**, 269 (2002).
[32]J. P. Biersack, Nucl. Instrum. Methods Phys. Res. B **35**, 205 (1988).
[33]E. H. Rhoderick and R. H. Williams, *Metal-Semiconductor Contacts* (Oxford Science, Oxford, 1988).
[34]V. Saxena, J. N. Su, and A. J. Steckl, IEEE Trans. Electron Devices **46**, 456 (1999).
[35]J. Sullivan, R. T. Tung, M. Pinto, and W. R. Graham, J. Appl. Phys. **70**, 7403 (1991).
[36]R. T. Tung, Phys. Rev. B **45**, 13509 (1992).
[37]H. J. Im, Y. Ding, J. P. Pelz, and W. J. Choyke, Phys. Rev. B **64**, 075310 (2001).
[38]L. D. Bell and W. J. Kaiser, Phys. Rev. Lett. **61**, 2368 (1988).
[39]M. O. Aboelfotoh, J. Appl. Phys. **66**, 262 (1989).
[40]R. F. Egerton, *Electron Energy-Loss Spectroscopy in the Electron Microscope*, 2nd ed. (Plenum, New York, 1996).
[41]H. Norde, J. Appl. Phys. **50**, 5052 (1979).
[42]F. Roccaforte, F. La Via, V. Raineri, L. Calcagno, and F. Mangano, Appl. Phys. Lett. **83**, 4181 (2003).
[43]J. A. Gardner *et al.*, J. Appl. Phys. **83**, 5118 (1998).
[44]F. Giannazzo, L. Calcagno, V. Raineri, L. Ciampolini, M. Cippa, and E. Napolitani, Appl. Phys. Lett. **79**, 1211 (2001).
[45]R. T. Tung, Mater. Sci. Eng., R. **35**, 1 (2001).
[46]P. Blood and J. W. Orton, *The Electrical Characterization of Semiconductors: Majority Carriers and Electron States*, edited by N. H. March (Academic, London 1992), p. 297.
[47]I. Pintilie, L. Pintilie, K. Irmscher, and B. Thomas, Appl. Phys. Lett. **81**, 4841 (2002).
[48]T. Dalibor, G. Pensl, H. Matsunami, T. Kimoto, W. J. Chokye, A. Schöner, and N. Nordell, Phys. Status Solidi A **162**, 199 (1997).
[49]J. H. Zhao, K. Sheng, and R. C. Lebron-Velilla, Int. J. High Speed Electron. Syst. (in press).
[50]H. C. Card and E. H. Rhoderick, J. Phys. D **4**, 1589 (1971).
[51]R. T. Tung, Mater. Sci. Eng., R. **35**, 1 (2001).
[52]C. Y. Wu, J. Appl. Phys. **51**, 4919 (1980).